Int J Biometeorol (1997) 41:5–12

ORIGINAL ARTICLE

Katrin Maak · Hans von Storch

Statistical downscaling of monthly mean air temperature to the beginning of flowering of *Galanthus nivalis* L. in Northern Germany

Received: 7 August 1996 / Accepted: 27 November 1996

Abstract We have examined the relationship between phenological data and concurrent large-scale meterological data. As phenological data we have chosen the beginning of the flowering of *Galanthus nivalis* L. (flowering date) in Northern Germany, and as large-scale meteorological data we use monthly mean near-surface air temperatures for January, February and March. By means of canonical correlation analysis (CCA), a strong linear correlation between both sets of variables is identified. Twenty years of observed data are used to build the statistical model. To validate the derived relationship, the flowering date is downscaled from air temperature observations of an independent period. The statistical model is found to reproduce the observed flowering dates well, both in terms of variability as well as amplitude. Air temperature data from a general circulation model of climate change are used to estimate the flowering date in the case of increasing atmospheric carbon dioxide concentration. We found that at a time of doubled CO_2 concentration (expected by about 2035) *G. nivalis* L. in Northern Germany will flower ~2 weeks and at the time of tripled CO_2 concentration (expected by about 2085) ~4 weeks earlier than presently.

Key words Plant phenology · *Galanthus nivalis* L. · Climatic effect of plant events · Statistical downscaling · Northern Germany

Introduction

Phenological data have been gathered on various plant species to study the seasonal timing of life cycle events (phases) (Schnelle 1955). The old practice provides a valuable source of information about ecosystems. Furthermore, phenological data are a powerful tool for monitoring the important relation between ecosystems and weather or climate. An important issue is the effect of human activities of the atmosphere and estimation of the possible consequences of climate change for ecosystems.

General Circulation Models (GCMs) are used to study global climate change. The typical grid sizes of these models are ~500 km; smaller scales cannot be resolved (Robinson and Finkelstein 1991). While GCMs are able to reproduce 'large-scale' climate information to a good level of approximation, there is general interest in finding a link between large-scale information and local parameters. This will offer the possibility of estimating local effects in the case of increasing atmospheric CO_2 concentration.

One way to solve this problem is the use of statistical downscaling. This method determines empirically a link between a large-scale and a local parameter. Currently, statistical downscaling is used to find the relationship between a climatological parameter and local ones such as temperature or precipitation. The goal of the present study is to investigate if it is possible to link a climatological parameter with a non-meteorological parameter such as the beginning of the flowering of a plant.

A condition for the application of the method is the existence of a long homogeneous time series needed to fit and confirm the statistical relationship. The statistical downscaling is subdivided into four steps (von Storch et al. 1993): (1) Find a large-scale parameter which controls the local parameter; a good simulation of the large-scale parameter in climate models is necessary to estimate the local parameter for future changes. (2) Set up a statistical relationship between these parameters. (3) Validation of that relationship with independent data. (4) Given a successful validation the local parameter can be estimated for future changes with the large-scale parameter derived from GCM experiments.

In the present paper the near-surface air temperature is taken as the large-scale parameter and the beginning of the flowering of *G. nivalis* L. (flowering date) as the local parameter. We have chosen results from 'time-slice experiments' (see detailed description of the experiment), conducted with a T42 atmospheric GCM (Cub-

K. Maak (✉) · H. von Storch
Institute for Hydrophysics, GKSS Research Centre,
21502 Geesthacht, Germany

asch et al. 1995) as scenarios for the expected times of doubled and tripled atmospheric CO_2 concentration. This yields the air temperature field which is used to estimate future changes for the flowering date.

The following report gives detailed information about the datasets used, including a description of the statistical model together with the fitting and validation of the model. The resulting flowering dates for Schleswig-Holstein are compared with observations from eastern England. The model is applied to interpret the time-slice GCM experiments for possible future changes of the flowering date. The paper concludes with a summary of the results and a discussion about the limitation of the downscaling model.

Data

Phenological data

In this work the collection of phenological data from the Deutscher Wetterdienst (DWD) is used. Since 1951 more than two hundred phases have been observed at 357 stations in Schleswig-Holstein (for location see Fig. 1). The phase coinciding with the beginning of flowering of *G. nivalis* L. (flowering data) is chosen to describe the first phenological season (Fig. 2). Spring flower phases are strongly influenced by the air temperature of the previous month (Defila 1992). Seventy-four stations with a 'homogeneous' spatial distribution are selected (Fig. 3, Table 1) and the '30-days-error' is corrected after visual comparisons of neighbouring stations where possible. (This relatively frequent error happens if the observer confuses columns in the record sheet, so that the flowering event is erroneously reported 30 days later or earlier). In this dataset there is no recognizable trend for the whole period from 1951 to 1990 (see Fig. 5). From 1971 to 1990 the observed dataset is almost complete and this period is chosen to establish the statistical relationship between flowering date and air temperature. The remaining data are used to validate the specified relationship.

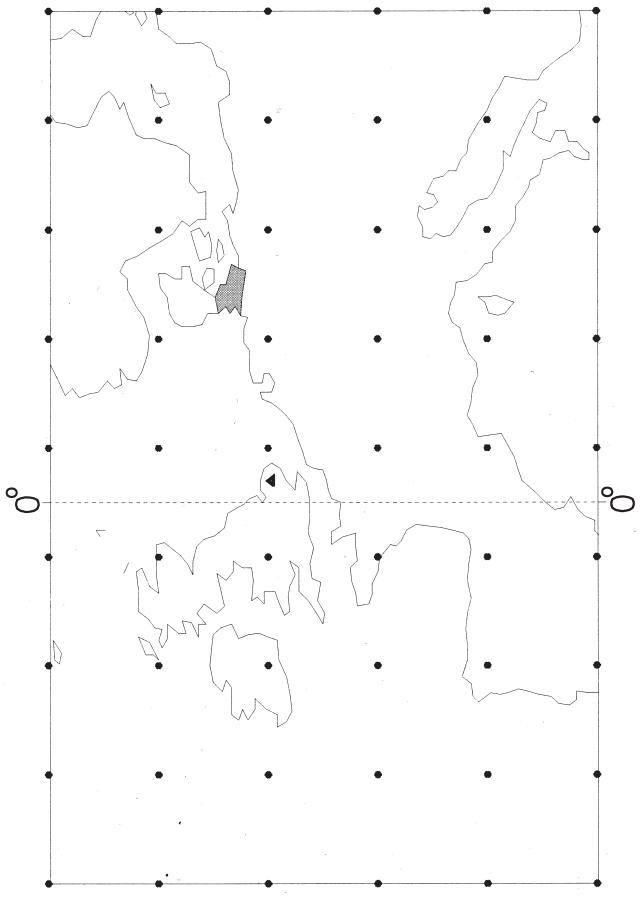

Fig. 1 Location of the datasets used. The *hatched region* shows the area of the 74 stations in Schleswig-Holstein, the *triangle* depicts the Marsham estate in Eastern England and the 5°×5° gridded air temperature observations (Jones and Briffa 1992) are indicated by *dots*

Air temperature data

We applied the gridded monthly 2 m-temperature based on observations for the years 1870 to 1990 compiled by Jones and Briffa (1992). The months January, February and March are used and a region is selected extending from 17.5°W to 22.5°E and from 37.5°N to 62.5°N (Fig. 1). The dataset is mostly homogeneous, although based on an increasingly denser observational network. For the following calculations we consider the concatenated January, February and March air temperature fields as one large vector. For representation, this vector is split again into three blocks, representing the January, February and March air temperatures.

Fig. 2 Flower of *Galanthus nivalis* L.

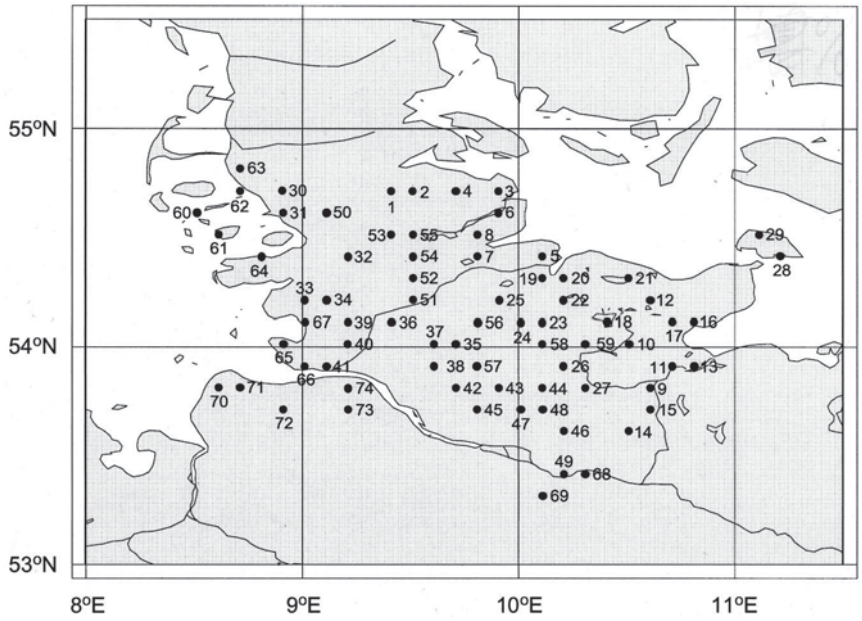

Fig. 3 Distribution of the 74 selected stations in Schleswig-Holstein

Table 1 The 74 stations and the local correlations between the estimated and observed flowering date anomalies for the validation period. For some stations, meaningful calculation of correlations is not possible, because of insufficient data. However, the stations have been used for the calculations of empirical orthogonal functions (EOF) and canonical correlation analysis (CCA)

1. Flensburg 0.63
2. Bistof 0.78
3. Gelting –
4. Sterup 0.78
5. Daenschenhagen 0.86
6. Schuby 0.96
7. Hohenlieth 0.75
8. Rieseby 0.82
9. Lübeck 0.78
10. Ahrensbök 0.59
11. Bad Schwartau 0.81
12. Benz 0.73
13. Niendorf –
14. Duvensee 0.93
15. Rondeshagen 0.78
16. Neustadt 0.68
17. Schönwalde 0.71
18. Pfingstberg 0.72
19. Kitzeberg 0.68
20. Klausdorf 0.59
21. Lütjenburg 0.97
22. Raisdorf 0.62
23. Obendorf/Wankendorf 0.72
24. Bordesholm 0.74
25. Schierensee 0.81
26. Fahrenkrug 0.86
27. Sühlen 0.70
28. Burg auf Fehmarn 0.79
29. Daenschendorf 0.72
30. Leck 0.77
31. Bredstedt 0.72
32. Hollbüllhuus –
33. Heide 0.69
34. Linden 0.42
35. Meezen 0.78
36. Osterholzteich 0.68
37. Lockstedt 0.79
38. Hohenlockstedt 0.83
39. Albersdorf 0.75
40. Burg –
41. St. Michelsdonn 0.77
42. Lutzhorn 0.81
43. Kaltenkirchen 0.92
44. Öring 0.76
45. Borstel-Hohenraden 0.95
46. Wulfsdorf 0.72
47. Harksheide 0.73
48. Wiemerskamp 0.76
49. Hamburg-Bergedorf 0.85
50. Jordelund 0.77
51. Hamdorf 0.82
52. Hohn 0.67
53. Jübek 0.86
54. Kropp 0.77
55. Lürschau 0.74
56. Nortorf 0.75
57. Bad Bramstedt 0.68
58. Rickling 0.62
59. Tensfeld 0.56
60. Wyk auf Föhr 0.42
61. Pellworm 0.81
62. Dagebüll –
63. Neukirchen 0.4
64. Norder-Hever-Koog 0.76
65. Friedrichskoog 0.55
66. Helse 0.67
67. Wöhrden 0.60
68. Niedermarschaft 0.5
69. Roydorf 0.69
70. Cuxhaven/Sahlenburg –
71. Altenbruch 0.76
72. Ihlienworth 0.52
73. Hüll 0.72
74. Öderquart –

Statistical downscaling

Canonical correlation analysis of the large-scale and the local parameter

The connection between the European air temperature for January, February and March and the flowering date was investigated by canonical correlation analysis (CCA). For the mathematics of CCA, refer for instance to von Storch (1995). Let $T(x,K)$ denote the monthly mean air temperature observed in the year K at the space-time gridpoint x, i.e. x runs through the air temperature observation stations and additionally for each such station, through the months January, February and March. The observations of the flowering date are denoted by $B(y,K)$, where y represents the stations and K the year. For the following calculations anomalies of these parameters with respect to the fitting period are applied.

Prior to CCA, the flowering date anomaly and air temperature anomaly fields are first truncated to an approximation by the first few empirical orthogonal functions (EOFs; see also von Storch 1995). In this procedure the 'characteristic structure' or 'main modes of variability' of the air temperature anomalies $T_S(x,K)$ and the flowering date anomalies $B_S(y,K)$ are separated from the noise and irrelevant details.

The CCA yields an expansion of the subspaces of these fields

$$T_s(x,K) = \sum_{i=1}^{z} (M_i(x) \cdot \alpha_i(K)) + \varepsilon \quad (1)$$

$$B_s(y,K) = \sum_{i=1}^{z} (N_i(y) \cdot \beta_i(K)) + \varepsilon', \quad (2)$$

where $M_i(x)$, $N_i(y)$ is the i-th 'CCA-pattern' and $\alpha_i(K)$, $\beta_i(K)$ the i-th 'CCA-time series'; z is the number of the retained patterns and time series; ε is the unexplained portion.

The time series fulfill the following orthogonality conditions:

$$\left\langle \vec{\alpha}_i, \vec{\alpha}_j \right\rangle = \left\langle \vec{\beta}_i, \vec{\beta}_j \right\rangle = \delta_{ij}$$
$$\text{and} \quad \left\langle \vec{\alpha}_i, \vec{\beta}_j \right\rangle = \delta_{ij} \cdot r_i, \quad (3)$$

with r_i describing the correlation between the pair of time series.

$\alpha_1(K)$ and $\beta_1(K)$ have the maximum possible correlation, $\alpha_2(K)$ and $\beta_2(K)$ have the next highest correlation by being orthogonal to the former pair, and so on.

The explained variance for each gridpoint x is defined as:

$$\eta(x) = 1 - \frac{\mathrm{Var}(T(x,K) - T_s(x,K))}{\mathrm{Var}\, T(x,K)} \quad (4)$$

A parameter to measure the 'importance' of a pattern is the amount of total explained variance

$$\eta_{\text{total}} = \frac{1}{L} \sum_{x=1}^{L} \eta(x), \quad (5)$$

with L denoting the number of the gridpoints x.

Estimating flowering dates from the large-scale parameter

To build up the downscaling model, the subspaces of the air temperature anomaly fields $\vec{T}_S$ and of the flowering date anomaly fields $\vec{B}_S$ are used. Let $\vec{T}'$ and $\vec{B}'$ be independent data, which are assumed to have the same main modes of co-variability as $\vec{T}_S$ and $\vec{B}_S$. By analogy with Eq. 1, $\vec{T}'_S$ is projected onto $M_i(x)$:

$$T'_S(x,K) = \sum_{i=1}^{z' \le z} (M_i(x) \cdot \alpha'_i(K)) + \varepsilon \quad (6)$$

The reduced number of the retained pattern and time series is indicated by z'.

The error ε is minimized by the least square method and a new time series α'_i is calculated. If $\alpha'_i(K)$ is correlated with $\beta'_i(K)$ in the same manner as $\alpha_i(K)$ and $\beta_i(K)$, it is possible to estimate $\beta'_i(K)$ according to Eq. 3:

$$\beta'_i(K) = r_i \cdot \alpha'_i(K) \quad (7)$$

Assuming that $\vec{B}'_S$ and $\vec{B}_S$ share the same $N_i(y)$ and disregarding ε provides an estimation for the anomaly of the flowering date:

$$\widehat{B'_S}(y,K) \approx \sum_{i=1}^{z'} (N_i(y) \cdot \widehat{\beta'_i}(K)) \quad (8)$$

Fitting and validating the statistical model

CCA between the air temperature and flowering date anomalies

Only the leading flowering date EOF-pattern and the leading three air temperature EOF-patterns are selected to represent the subspaces of the parameters. These patterns explain 82% of the air temperature and 72% of the flowering date variance for the years 1971–1990.

The higher indexed patterns are disregarded:

1. For the air temperature, each describes <5% of the variance and hence these patterns are not important for the characteristic structure.
2. In the case of the flowering date they show a more complex structure. Only at a few individual stations can the signal be relevant.

The CCA between these subspaces of the parameters show a strong connection, with a correlation of 0.96 (Fig. 4). The CCA-pattern of the air temperature is positive everywhere with maximum values of 2.4° C over central and eastern Europe and minimum values of 0.3° C over the North Atlantic and the Mediterranean. Thus a gradient between maritime and continental influenced regions is recognized. The explained variance amounts of 60%. The CCA-pattern of the flowering date shows a uniform field of early flowering dates with amplitudes in the range of –6 to –20 days and explains 72% variance.

As the associated CCA-time series are normalized, the characteristic amplitudes result from the patterns. The typical flowering date anomaly is 13 days. If an air temperature field, as in Fig. 4, right, is assumed for January, February and March in a particular year, the average flowering date is 13 days earlier than 'normal'. Equally a negative air temperature field with the same strength means an average delay in flowering date of ~13 days. It is worth mentioning that the air temperature CCA-pattern is very similar to the first EOF-pattern of the air temperature.

These results and considerations indicate the possibility for estimating the flowering date variations from the climatological air temperature fields.

Validating the estimated flowering date with observational data

To verify the link found in the previous section the flowering date anomalies are estimated from the independent air temperature anomalies for the years 1870 to 1970 using Eqs. 6, 7 and 8. These estimated flower data are compared with the observed data from the DWD for the years 1951 to 1970. In Fig. 5 the means from all stations of the estimated and observed flowering date anomalies are shown. The correlation between these datasets is 0.74. The local correlations for each of the 74 stations are calculated (Table 1), of which some are very

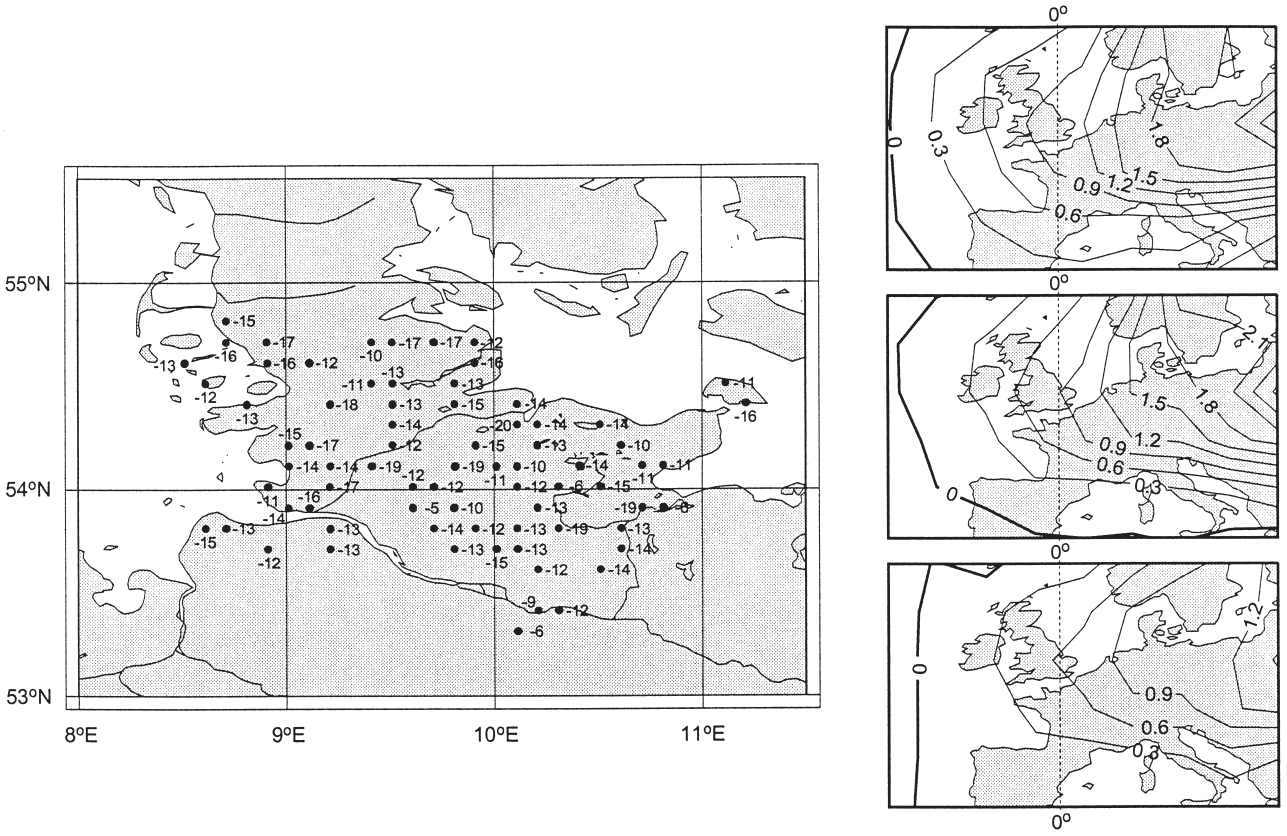

Fig. 4 First pair of canonical correlation patterns of the flowering date and the monthly mean air temperature for January, February and March (from top to bottom) for the years 1971–1990. The flowering date anomalies are given in days and the air temperature anomalies for each month in °C; the coefficient times series are correlated with r=0.96

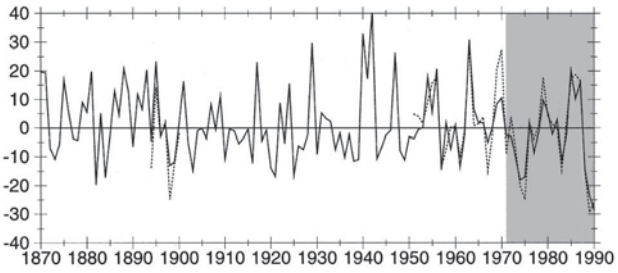

Fig. 5 Air temperature observations for 1870–1970 are downscaled to derive flowering date anomalies (*solid line*). These are compared with flowering date observations (*dashed lines*) from the Deutscher Wetterdienst for the years 1951–1970 and from Knuth for the years 1894–1900. Furthermore the fitting period (1971–1990) is added (*shaded* area). The time series depict anomalies in days

high and others rather low. In Fig. 6 two stations are selected to depict a less good correlation (Niedermarschaft, station 68, with a correlation of only 0.5) and a good match (Fahrenkrug, station 26, with a correlation of 0.86) (for location see Fig. 3). The similarity at Fahrenkrug is very good and at Niedermarschaft is still reasonable.

For further verification the flowering date observations are available for 20 stations in Northern Germany from 1894 to 1900 (Knuth 1894, 1895, 1896–1899; Hahn 1900). Since these stations are not the same as the modern ones, we show the recorded and downscaled flowering date anomalies averaged over all stations in Fig. 5. The estimated and observed variations at the end of the last century fit remarkably well.

Applicability to other places

Flower observations were made by the Marsham family (Sparks and Carey 1995) from the village Stratton Strawless, Norfolk, Eastern England (for location see Fig. 1). The date are compared with the estimated flowering date anomalies for the time interval 1870–1958, for which we have both air temperature data and flowering dates (Fig. 7).

The Marsham flowering date anomalies fit well with the estimated anomalies after ~1915 (with a correlation of 0.68), but before 1915 the similarity between recorded and estimated flower data is marginal. We suggest that the observational routine in Marsham may have undergone some changes in 1915 and that the observed plants may have been located so that they have responded mainly to specifically local conditions. We conclude in this case that the distance between Eastern England and Northern Germany is small compared with the spatial scale of atmospheric processes influencing the flowering date variations. This finding supports our choice of the large-scale air temperature field as ‘predictor’ of the flowering date.

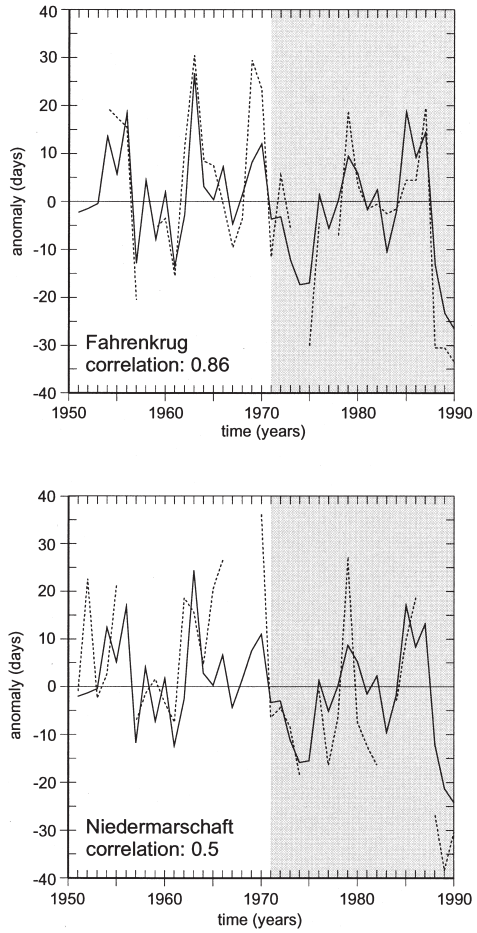

Fig. 6 Estimated (*solid line*) and observed (*dashed line*) flowering date anomalies for two selected stations, showing a good and a less good correlation

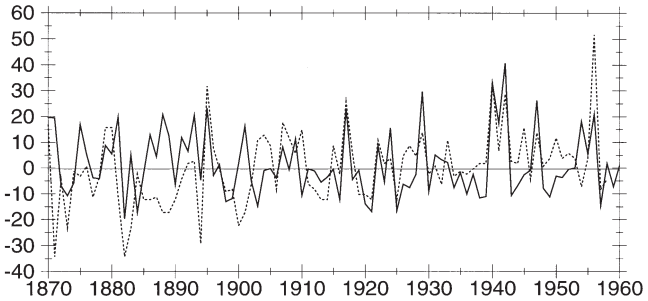

Fig. 7 Estimated historical flowering date variations (*solid line*) compared with the Marsham flowering date variations (*dashed line*) from Eastern England (for location see Fig. 1). The time series depict anomalies in days

Example of downscaling GCM data

Time-slice experiment

GCM air temperature data are selected from the results of three 'time-slice' experiments (Cubasch et al. 1995). Such numerical experiments are used to 'downscale' large-scale climate change information from a standard coarse-grid fully coupled atmosphere-ocean climate model, integrated with constant or continuously increasing greenhouse gas concentrations, to a small scale. For that purpose, the sea surface temperature and sea ice distributions from the coarse grid model are selected for certain times, and used as lower boundary conditions in a high-resolution atmosphere-only circulation model. This atmoshere-only model is then run with greenhouse gas concentrations specified according to the selected time-slices, so that the atmosphere equilibrates to the specified lower boundary conditions and greenhouse gas concentrations. The system is corrected for systematic errors in the sea surface temperature and sea ice distributions, as found in the base run under present conditions.

This procedure has the advantage that atmospheric information is generated on relatively small scales. The alternative, to run the high-resolution atmospheric model and the ocean model under 'transient', i.e. continuously changing greenhouse gas concentrations, is not feasible to date simply because of the computational costs.

We use the data from the high-resolution atmosphere model as input for our statistical downscaling model. Thus, our approach features two consecutive downscaling steps, with a dynamical model to downscale from global scale information to regional European-scale air temperature, and as second step the statistical model to derive from the European-scale air temperature field flowering dates for Northern Germany.

In the present case, the base climate model operates with a 'T21' horizontal resolution, corresponding to a mesh size of approx. 500 km, and is forced with a continuous increase of greenhouse gas concentrations of ~1% per year (Cubasch et al. 1992). This is the 'business-as-usual' scenario described by the International Panel on Climate Change (IPCC 1990). The 'high-resolution' is 'T42' with a mesh size of approx. 250 km. The three times slices chosen are: present conditions, doubling, and tripling of carbon dioxide concentrations in the simulation decades 2030–40 and 2080–90. All integrations were conducted for 30 years. This yields a significant increase of the European air temperature field for January, February and March (Cubasch et al. 1995). The mean air temperature field for the 30 winter seasons (January, February and March) increase by 1.2° C at the time of doubled CO_2 concentration and at the time of tripled CO_2 concentration by ~2.6° C. The air temperature anomalies for the $2{\cdot}CO_2$ and $3{\cdot}CO_2$ experiments are obtained by calculating the differences from the long-time mean of the 'control' experiment (i.e. with present day lower boundary conditions and greenhouse gas concentrations).

Estimated future flowering date anomalies

The European-scale air temperature anomalies from the 30 winter seasons obtained in the doubled and tripled carbon dioxide concentrations integrations are used for

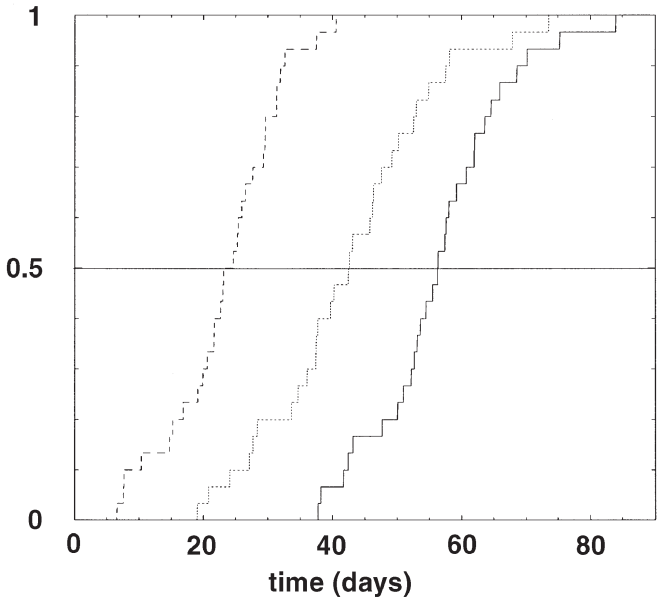

Fig. 8 Cumulative frequencies for the estimated flowering date from the air temperature of Jones and Briffa (1992; *solid line*), the doubled CO_2 (*dotted line*) and the tripled CO_2 time-slice experiment (*dashed line*)

estimating plausible future flowering dates according to Eqs. 6, 7 and 8. Thus, 30 flowering date estimates are generated for the two scenarios. The results averaged over all stations are shown as cumulative frequencies in Fig. 8. The estimated flowering dates from the observed air temperature anomalies for the years 1951–1980 is added. In the present day climate, half of the flowering dates are found before 28 February. The calculations yield that at the time of doubled CO_2 concentration the average flowering date is 2 weeks (13 February) and at the time of tripled CO_2 concentration >4 weeks (25 January) earlier than the present-day flowering date.

Summary and discussion

The canonical correlation analysis reveals a strong connection between the large-scale air temperature for January, February and March and the regionally influenced flowering date. A physiologically plausible explanation of this behaviour of the variables is obvious: positive air temperature anomalies lead to an early flowering date and negative air temperature anomalies result in a late flowering date. The derived downscaling model is able to reproduce flowering date anomalies with good correspondence to the observed ones. Additionally, a comparison of the downscaled historical flowering date anomalies and the observed dataset from Eastern England shows that the flowering date is controlled by the chosen large-scale air temperature field as climatological parameter field. Therefore flowering date anomalies may be derived from GCM air temperature data.

The average flowering date on the 13 February in the 'doubled CO_2' scenario is within ±1 standard deviation of the observed flowering date for the last decades. Thus the results of the doubled CO_2 scenario are convincing and can be viewed as plausible.

However for the 'tripled CO_2' scenario, the average flowering date is found to be outside 2 standard deviation interval of the observed data, so that we have to ask ourselves whether the statistical downscaling model is still valid.

First of all, to deal with the scenario of tripled CO_2, it may be useful to modify the statistical model so that it takes into account not only the air temperature conditions in January, February and March but also in December. Furthermore, we have to consider the plant physiological arguments to assess the reliability of this result. The flowering event represents the transition from the vegetative to the generative state, which is controlled by the seaonsal timing of air temperature. Thus the correct 'interpretation' of the temperature rise as the beginning of spring is an important requirement for the formation of the flowering date. For such an early date as 25 January, or even as early as 6 January (see Fig. 8), it is questionable whether there are changes in the plant behaviour by other influencing parameters. In the current climate the precipitation has only a small effect on the flowering date. For climate change scenarios precipitation might have a bigger influence. When we take into account that the mean flowering date is 1 month earlier in the UK than Northern Germany, the flowering date seems not to be limited by other parameters. Therefore the air temperature could still be an adequate predictor in the tripled CO_2 scenario.

Acknowledgements We would like to thank Hartmut Scharrer from the Deutscher Wetterdienst Zentralamt in Offenbach for preparation of the phenological data of Schleswig-Holstein. For kind permission to use the T42 time-slice experiments, we are grateful to Ulrich Cubasch and Jan Perlwitz. Also, we thank Tim Sparks for the Marsham *G. nivalis* L. data from Eastern England. Further thanks are due to Marion Grunert for the informative figures and Ralf Mohr for the photo of the flower of *G. nivalis* L. Moreover we are indebted to the Max-Planck-Institut für Meteorologie, where most of the work was done in a pleasant and inspiring scientific environment. Financial support was given by Bundesministerium für Bildung und Forschung, project 07VKV01/1.

References

Cubasch U, Hasselmann K, Höck H, Maier-Reimer E, Mikolajewicz U, Santer BD, Sausen R (1992) Time-dependent greenhouse warming computations with a coupled ocean-atmosphere model. Clim Dyn 8:55–69

Cubasch U, Waskiwitz J, Hegerl G, Perlwitz J (1995) Regional climate changes as simulated in time-slice experiments. Clim Change 31:273–304

Defila C (1992) Schweizerische Rundschau für Medizin. Schweiz Meteorol Anstalt, Zürich 11:343–346

Hahn A (1990) Phänologische Beobachtungen in Schleswig-Holstein im Jahre 1900. Schriften Naturwiss Vereins Schleswig-Holstein 12:309–315

IPCC (1990) Climate change – the IPCC scientific assessment. Houghton JT, Jenkins GJ, Ephraums JJ (eds). Cambridge University Press, Cambridge, UK

Jones PD, Briffa KR (1992) Global surface air temperature variations during the twentieth century: part 1. Spatial, temporal and seasonal details. The Holocene 2,2:165–179

Knuth P (1894, 1895) Phänologische Beobachtungen in Schleswig-Holstein im Jahre 1894 und 1895. Heimat 5:66–71 and 6:30–37

Knuth P (1896–1899) Phänologische Beobachtungen in Schleswig-Holstein im Jahre 1896, 1897, 1898 und 1899. Schriften Naturwiss Vereins Schleswig-Holstein 11:157–185, 252–259; 12:22–28, 51–57

Robinson PJ, Finkelstein PL (1991) The development of impact-oriented scenarios. Bull Am Meteorol Soc 4:481–490

Schnelle F (1955) Pflanzen-Phänologie. Geest and Portig, Leipzig

Sparks TH, Carey PD (1995) The responses of species to climate over two centuries: an analysis of the Marsham phenological record, 1737–1947. J Ecol 83:321–329

von Storch H (1995) Spatial patterns: EOFs and CCA. In: von Storch H, Navarra A (eds) Analysis of climate variability: applications of statistical techniques. Springer, Heidelberg New York, pp 227–258

von Storch H, Zorita E, Cubasch U (1993) Downscaling of global climate change estimates to regional scales: an application to Iberian rainfall in wintertime. J Climatol 6:1161–1171